THE ASTROPHYSICAL JOURNAL, 165:67–86, 1971 April 1

ABUNDANCE ANALYSES OF POPULATION II VARIABLE STARS
I. W VIRGINIS*

TIMOTHY BARKER, LEONA D. BAUMGART, DENNIS BUTLER, KYLE M. CUDWORTH, EDWARD KEMPER, ROBERT P. KRAFT,† JEAN LORRE, N. KAMESWARA RAO, GLENN H. REAGAN, AND DAVID R. SODERBLOM
Lick Observatory, Board of Studies in Astronomy and Astrophysics, University of California, Santa Cruz
Received 1970 November 5

ABSTRACT

From curve-of-growth analysis, abundances (relative to the Sun) of spectroscopically conspicuous metallic elements have been estimated in the archetypal Population II Cepheid W Virginis. The Fe abundance was confirmed by the use of fine analysis based on LTE model atmospheres. The mean metallic abundances, derived from three spectrograms well distributed in temperature around the cycle, are $[N_{\text{non-}s}] = -1.1$ and $[N_s] = -2.2$, where "s" refers to elements produced by the s-process and "non-s" to all other species. It is likely that the excessive metal deficiency of s-process elements reflects the composition of the primeval interstellar medium out of which W Vir was formed.

It is shown that the reduction in the metal/hydrogen ratio to one-tenth of the solar value leads to an affirmative test of the shock-wave model for the pulsations.

I. INTRODUCTION

Renewed interest in the chemical composition and atmospheric parameters of Cepheids in globular clusters has resulted from recent calculations of the late stages of stellar evolution. Schwarzschild and Härm (1970) showed that a star on the asymptotic red-giant branch could make loops to the left in the H-R diagram as a consequence of helium ignition. Of the stellar models considered, only those with high helium content ($Y = 0.30$) and low mass ($\mathfrak{M} = 0.65\ \mathfrak{M}_\odot$) were found to cross the Cepheid instability strip, a result independent of the choice of metal abundance ($Z = 0.001$ or 0.0001). High helium and low metal abundance also seem to be characteristic of Christy's (1966) pulsational model of the brightest field Cepheid of Population II, viz., W Virginis; and a large value of Y was found by Wallerstein (1959*b*) in his rough determination of the H/He ratio, based on emission lines, in the atmosphere of the same star. It is also known empirically that long-period Cepheids never occur in globular clusters of high metal content (Kwee 1968; Wallerstein 1970), i.e., presumably those with $Z > 0.001$.

However, few if any direct spectroscopic analyses of metal abundances in field Cepheids of Population II have been carried out. Rodgers and Bell (1963) studied the bright southern Cepheid κ Pav, but this star may not be characteristic of the globular-cluster population. Here we treat the archetypal object W Vir in coarse (curve of growth) and fine (LTE model atmosphere) analysis.

In his classical paper on W Vir, Abt (1954) assigned the hydrogen/metal ratio (essentially the solar value), derived from coarse analysis the atmospheric temperatures, pressures, and opacities, and used these to test the shock-wave model for the pulsations. In this paper, we shall proceed in reverse order; i.e., from estimates of the temperature, we shall use curves of growth to derive abundances, opacities, and pressures. We shall show, contrary to Abt's conclusion, that a shock-wave very satisfactorily represents the physical state of the atmosphere during the pulsation.

* *Contributions from the Lick Observatory*, No. 324.

† Visiting Fellow, Joint Institute for Laboratory Astrophysics, University of Colorado, 1970 July–December, where a portion of this work was completed.

II. COARSE ANALYSIS

a) Temperature Determinations

In the spectra of stars in the temperature range exhibited by W Vir, roughly 4000°–6500° K, lines of Fe I are displayed in such profusion and over such a wide range of intensities that coarse analyses are usually based upon them. Our treatment is no exception. Using the notation $[X] = \log X_*/X_\odot$ and adopting the Milne-Eddington approximation, we write

$$[N_{\text{Fe I}}] \equiv \left[\frac{N_{\text{Fe I}}}{V\kappa_\lambda}\right] + [V] + [\kappa_\lambda] , \tag{1}$$

where $[N_{\text{Fe I}}/V\kappa_\lambda]$ is the difference in abscissa between the stellar and solar curves of growth for Fe I, $[V]$ the difference in ordinate (i.e., difference in microturbulent velocity), $[\kappa_\lambda]$ the difference in mass absorption coefficient at a reference wavelength λ near the middle of the spectral region under consideration, and $[N_{\text{Fe I}}]$ the relative abundance of Fe I per gram of stellar material. From the horizontal and vertical shifts of the stellar and solar curves of growth, we derive $[N_{\text{Fe I}}/V\kappa_\lambda]$ and $[V]$, respectively. The determination of the Fe I abundance in the star therefore depends on estimating the continuous opacity, a known function of the ionization temperature T_{ion} and the electron pressure P_e. (In the present case, the principal sources of continuous opacity are free-bound and free-free transitions of H, H^-, and Rayleigh scattering on H.) From the horizontal shift of the stellar curve of growth for Fe II onto that for Fe I, one condition on T_{ion} and P_e is imposed by the Saha equation. A second condition could presumably be found from some other element manifesting itself in two ionic stages, e.g., Ti or Cr. For $T_{\text{ion}} \gtrsim 5000°$ K, however, the near equality of the first ionization potentials for elements in the iron-peak group renders this method indeterminate, and recourse must be had to estimating T_{ion} from some other consideration.

In his study of several RR Lyrae stars, Preston (1961), for example, estimated T_{ion} from T_{exc}, the latter being defined (through the Boltzmann equation) as that temperature giving the best fit of the Fe I lines to an appropriate theoretical curve of growth for the star. Oke and Searle (1962), Searle, Oke, and Giver (1962), Gunn and Kraft (1963), Searle and Rodgers (1966), Oke (1966), and others made use of profiles of Hγ to obtain temperatures for various F-type stars, variable and non-variable. In the present work, we are able to estimate T_{ion} by three different methods, but the use of the wings of Hα is taken as fundamental.

Our observational material consists of the twenty-three spectrograms obtained in the conventional photographic blue by R. F. Sanford and H. A. Abt at the coudé spectrograph of the Mount Wilson 100-inch telescope between 1948 and 1951, and sixteen spectrograms of W Vir and several MK supergiants of spectral types F and G obtained by us with the coudé spectrograph of the 120-inch Lick reflector. The Mount Wilson spectrograms have a dispersion of 10 Å mm^{-1}, and the reader is referred to the paper by Abt (1954) for observational details. The Lick spectrograms, listed in Table 1, cover a 300 Å interval including Hα and were obtained on Eastman 103a-D emulsion with a Varo-type image tube mounted at the 20-inch camera; the dispersion was 15 Å mm^{-1}. The projected slit width, as judged from microphotometer tracings of weak comparison lines, is 0.6 Å, i.e., 27 km sec^{-1} at Hα, a value about 1.3 times greater than the resolution of the particular camera/plate combination when used in unaided form.

We reanalyzed the Mount Wilson material for line intensities of conspicuously identifiable metallic elements and reconstructed Abt's curves of growth, using the Hα observations as a basis for temperature determination. However, since the hydrogen lines of W Vir are in emission from phase $0.65P$ to $0.10P$ (counted from photographic light maximum), it was necessary to select a phase of W Vir for Hα observations which satisfied three conditions: (1) hydrogen lines fully in absorption, (2) W Vir not so cool that

TABLE 1

WIDTHS OF Hα [$W(0.90)$] FOR W VIRGINIS AND MK SUPERGIANTS

Star	Sp. Type	Plate No. (Lick Coudé)	Date (1970 UT) (mid-exp.)	$W(0.90)$ (Å)
HD 161796...	F3 Ib	EC 8531	April 24.430	10.7
35 Cyg.....	F5 Ib	EC 8540	April 24.478	12.0
41 Cyg.....	F5 Ib	EC 8541	April 24.521	12.5
HR 7308.....	F6 Ib–II	EC 8539	April 24.513	8.9
45 Dra.....	F7 Ib	EC 8534	April 24.567	6.6
γ Cyg	F8 Ib	EC 8542	April 24.526	8.9
HR 7008.....	F9 Ib	EC 8535	April 24.453	7.5
ε Leo.....	G0 II	EC 8517	April 24.221	5.3
β Dra.....	G2 Ib	EC 8530	April 24.428	4.5
ζ Mon.....	G2 Ib	EC 8516	April 24.226	5.2
ξ Pup.....	G3 Ib	EC 8513	April 24.207	5.7
ε Gem.....	G8 Ib	EC 8512	April 24.188	2.9
W Vir.....	G I(pec)	EC 8562	May 20.219	2.3*
W Vir.....	G I(pec)	EC 8563	May 20.309	2.3
W Vir.....	G I(pec)	EC 8567	May 21.182	2.3
W Vir.....	G I(pec)	EC 8568	May 21.207	2.7

* Half-weight.

the wings of the hydrogen lines are no longer sensitive to temperature, and (3) proximity in phase to a Mount Wilson plate of high quality. These conditions were met on 1970 May 20 and 21 UT when four Hα spectrograms were obtained at a mean phase of $0.46P$. Abt's excellent spectrogram taken at phase $0.40P$ (Ce 7010) was therefore adopted as the basic plate from which metal abundances were to be estimated. The propriety of using Hα rather than one of the other hydrogen lines as a temperature indicator will be readily understood from visual inspection of the Mount Wilson spectrograms. At phases when conditions (1) to (3) above are satisfied, the wings of Hβ, Hγ, and Hδ are cluttered with metallic lines and cannot be reliably measured; interference of this kind is minimal at Hα.

The width $W(0.90)$ of Hα at residual intensity 0.90 was measured for each of the MK supergiants; values of this quantity are listed in Table 1 and plotted against spectral type in Figure 1. Following Rodgers and Bell (1967), Schmidt (1970) has calculated Hα line profiles and corresponding values of $W(0.90)$ as a function of surface gravity g and effective temperature T_e from flux-constant model atmospheres in LTE. According to Parsons and Bouw (1970), these stars have $\log g \approx 1$–1.5; in Figure 1 we plot, as a function of spectral type, the values of T_e derived from Schmidt's calculation for the observed values of $W(0.90)$ and $\log g = 1$. Also shown in Figure 1 is the (spectral type, T_e)-relationship derived by Parsons and Bouw (1970), from a fit of model atmosphere fluxes to six-color photometry. This has been extended later than G3 Ib by using Kraft's (1961) calibration, with which it differs only slightly.

Inspection of Figure 1 reveals the following: (1) For stars earlier than about G2 Ib, $W(0.90)$ is a very satisfactory indicator of effective temperature; a single measurement yields a value of T_e with a probable error of $\pm 150°$ K, given the broadening theory. (2) The temperature difference between the two broadening theories declines with advancing spectral type. (3) For stars earlier than G2 Ib, the Hα measurements give essentially the same values of T_e as the Parsons-Bouw-Kraft scale. Later than G2 Ib, however, the scales separate in the sense that the widths of Hα give higher temperatures. This may be readily understood in the light of work by Kraft, Preston, and Wolff (1964), who showed that the Doppler core of Hα becomes very wide in the spectra

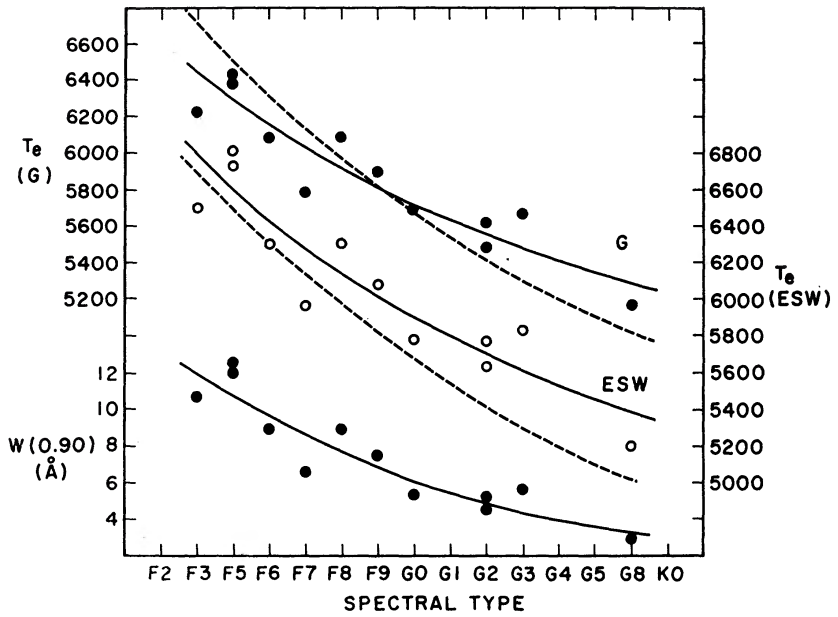

FIG. 1.—Effective temperatures derived from $W(0.90)$ for the supergiants in Table 1. From bottom to top, the observed spots and freehand solid curves fitted to them represent: (1) $W(0.90)$, the width of Hα at a residual intensity 0.90, corrected for instrumental width; (2) values of T_e derived from $W(0.90)$ and Schmidt's (1970) calculation based on the broadening theory of Edmonds *et al.* (1967); (3) the same, based on the broadening theory of Griem (1964), all as a function of spectral type. Dashed curves represent the (T_e, spectral type)-relation according to Parsons and Bouw (1970) and Kraft (1961).

of stars of advancing spectral type, and satisfies a relationship between core width and absolute magnitude analogous to the well-known Wilson-Bappu (1957) effect. In stars later than G2 Ib, the wings of the hydrogen lines are distorted by a powerful Doppler core arising high in the atmosphere (Kraft, Preston, and Wolff 1964), for which the line-formation theory does not adequately account. What Figure 1 demonstrates is that, for stars not having a wide Hα core, $W(0.90)$ can be used to estimate reliable values of T_e.

The four Hα spectrograms of W Vir yield a mean value $W(0.90) = 2.4 \pm 0.12$ (p.e.) Å, corrected for instrumental width, at a mean phase of $0.46P$. Hα is narrower in W Vir than in any standard star listed in Table 1. At this phase Abt (1954) gives a value of $T_{\rm ion} = 5320°$ K based on solar metal abundances. Since $T_e \geqq T_{\rm ion}$, the equivalent Population I spectral type is not later than G3 Ib. However, the observed width of Hα in W Vir corresponds to a star of much lower effective temperature, and suggests that (1) for some reason W Vir does not share in common with Population I supergiants a wide Doppler core in Hα and (2) the metal/hydrogen ratio is smaller than the solar value.

At phase $0.46P$, W Vir achieves approximately its maximum photospheric radius, and $\log g \sim 0$ (see § IV). According to Schmidt (1970), $W(0.90)$ shows an inverse effect with $\log g$; extrapolating his results from the $\log g = 2$–1 range, we find that the value of T_e increases about 200° K in passing from $\log g = 1$ to $\log g = 0$. Fine analysis (§ III) indicates that the lower metal abundance in W Vir leads to a slight reduction in $\log P_e$ at the optical depths where the wings of Hα are formed; this simulates a small increase in the surface gravity. The net effect of the two corrections is to reduce the value of T_e about 100° K below the prediction of Schmidt's calculation for $\log g = 1$. Taking a mean of the Griem (1964) and Edmonds, Schlüter, and Wells (1967) broadening theories, we derive $T_e = 4880°$ K at phase $0.46P$.

Further support for the applicability of Schmidt's results to W Vir is found in Figure 2, where observed profiles of Hα for W Vir and for the field Population I supergiant ϵ Gem (G8 Ib) are exhibited. In W Vir the wings of Hα are symmetrical but in ϵ Gem are not, and an average profile for the two sides of the line is illustrated. A small extrapolation of temperature from Schmidt's calculations yields the computed profile for T_e = 5050° K and log g = 1; it is a good match to Hα in W Vir. Yet in ϵ Gem the enormous Doppler core of the observed line renders it astonishingly dissimilar to its theoretical counterpart, even though T_e = 5080° K (Kraft 1961) and log $g \sim 1$ (Parsons and Bouw 1970) for this star. We note that other combinations of log g and T_e differing from the above by one order of magnitude and $\pm$ 200° K, respectively, would also give a satisfactory fit to the profile of Hα in W Vir. However, since we wish to determine the correct order of magnitude of the metal/hydrogen ratio in the coarse analysis, we are satisfied with a determination of T_e correct to this kind of precision; a change in T_e of 200° K corresponds to a change in $[N_{Fe}]$ of 0.3. The above numbers would be modified only slightly if a Griem profile were substituted for the ESW profile in Figure 2.

From the slope of Abt's (1954) T_{exc} or T_{ion} curve at phase 0.46P, we estimate that at phase 0.40P, when plate Ce 7010 was obtained, T_e = 5050° K and T_{ion} = 4800° K. To these values we give the highest weight.

A second method for estimating T_{ion} is the use of Preston's (1961) numerical "device," which is based on experience with analyses of numerous F- and G-type stars of normal metal abundance, viz., $\theta_{ion} = \theta_{exc} - 0.15$, where $\theta = 5040/T$. From the Fe I curve of growth for Ce 7010 (see § II*b*) we obtained T_{exc} = 4040° K in agreement with Abt's result; thus T_{ion} = 4580° K.

The preceeding values of T_{ion} are low enough that the Boltzmann factor in the Saha equation is fairly sensitive to small changes in first ionization potential among iron-peak elements. Thus, as a third method, we have estimated T_{ion} (and log P_e) from a comparison of the abscissae of the Fe II and Fe I curves of growth with those of two corre-

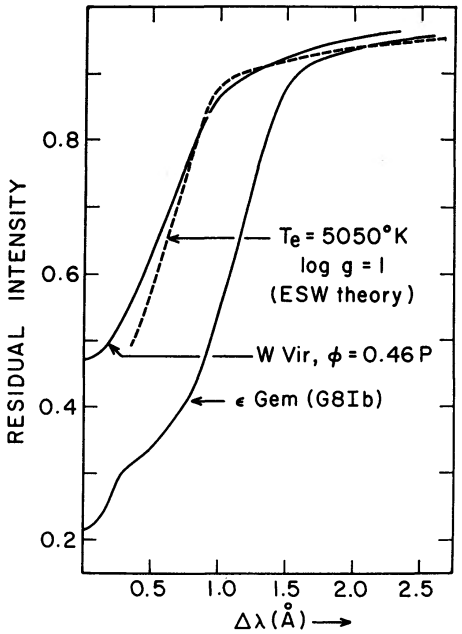

FIG. 2.—Observed profiles of Hα for supergiants with T_e near 5000° K, compared with a theoretical profile for T_e = 5050° K, log g = 1. The latter is taken from calculations by Schmidt (1970), based on ESW broadening theory.

sponding ionization stages in Ti and Cr. Since Cr I and Cr II lines differ rather markedly in mean excitation potential and mean line strength, Cr is less satisfactory for the purpose than Ti. For Ce 7010, the plot of Ti versus Fe lines yields $T_{\rm ion} = 4600°$ K whereas for Cr versus Fe, $T_{\rm ion} = 3770°$ K; to these we assign relative weights of 2 and 1, respectively.

In Table 2, we summarize the methods used to obtain $T_{\rm ion}$ in W Vir at phase 0.40 P. The weighted mean is $4590° \pm 320°$ K (m.e.). Some justification for the physical reality of the construct $T_{\rm ion}$ and for the use of numeral "devices" taken over from stars of normal metal abundance to metal-poor stars will be offered in the Section on fine analysis (§ III).

b) Curves of Growth; Abundances

Curves of growth for Fe I and Fe II were constructed for sixteen different spectra of W Vir, well distributed in phase, on fifteen of the twenty-three Mount Wilson spectrograms; on one plate showing double lines, it was possible to analyze both spectra. The equivalent widths were those published by Abt (1954), except that lines shortward of 4100 Å were generally omitted on the grounds that the continuum location is rather uncertain. Solar log η's taken from the lists by Preston (1961) and Gunn and Kraft (1963) were used; solar log η's not given by them were read directly out of the solar curve of growth (Goldberg and Pierce, in Aller 1953) by using line strengths taken from the Utrecht Photometric Atlas. Corresponding corrected stellar log η's were obtained from $\log \eta_* = \log \eta_\odot + \chi((\theta_{\rm exc})_\odot - (\theta_{\rm exc})_*)$, in intervals of 0.05 in $(\theta_{\rm exc})_\odot - (\theta_{\rm exc})_*$, where χ is the excitation potential of the lower level of each transition. That $(\theta_{\rm exc})_*$ was adopted which gave a curve of growth ($\log \eta_*$ versus $\log [W/\lambda]$) having the least systematic displacement between lines of high and low excitation. Our values of $(\theta_{\rm exc})_*$ differed from Abt's (1954) generally by no more than 0.05; exceptions were found for plates Ce 7091 and Ce 5058, both of which are spectrograms of comparatively low quality. Abt's values and ours were averaged, a smooth curve was passed through a plot of $(\theta_{\rm exc})_*$ versus phase, and a "smoothed" value of $(\theta_{\rm exc})_*$ was assigned to each plate. These are listed in Table 3 along with values of the microturbulent velocity [V]. We took $(\theta_{\rm exc})_\odot = 1.04$ (Preston 1961) and $V_\odot = 2.3$ km sec^{-1}.

We note that the mean $T_{\rm ion}$ for Ce 7010 derived from the independent methods discussed in § II*a* satisfied exactly Preston's "device." We therefore apply the "device" to all other phases of W Vir, deriving the values of $(\theta_{\rm ion})_*$ given in Table 3. Iron abundances were then obtained for all plates from the shift of the Fe II onto the Fe I curve of growth, the calculation of the continuous opacity, and the application of equation (1). We adopted $(\theta_{\rm ion})_\odot = 0.89$ at a representative solar optical depth of $\tau = 0.35$ (Aller and Pierce 1952) and $\log (\kappa_\lambda)_\odot = -0.47$ at $\lambda = 4550$ Å, a point midway in the region of spectral analysis. The degree of ionization of Fe I is high at all phases, and essentially all Fe is Fe II. At phases near maximum light exhibiting double lines, the abundance of Fe was obtained for one or both spectra whenever the number of lines was sufficiently large to

TABLE 2

ESTIMATES OF $T_{\rm ion}$ AT $\phi = 0.40\ P$ (Ce 7010)

Method	$T_{\rm ion}$ (° K)	Weight
1) Hα width	4800	1
2) Ti versus Fe	4600	$\frac{1}{2}$
3) Cr versus Fe	3770	$\frac{1}{4}$
4) $T_{\rm exc} \rightarrow T_{\rm ion}$ (Preston's "device")	4580	$\frac{1}{4}$
Weighted mean	4590±320 (m.e.)	

TABLE 3

RESULTS FROM CURVES OF GROWTH

Plate Ce	Phase (0.000 = max.photo-graphic)	Com-ponent	θ^*_{exc} (observed)	θ^*_{ion} (smoothed)	[V] (from Fe I)	log a (from Fe I)	No. Fe I lines measured	$[N_{Fe}]$
5110	0.650	-	1.465	1.315	+0.39	-2.4	53	-1.4
7080	0.709	L	1.39	1.24	+0.26	-1.8	42	-1.3
7085	0.767	L	1.29:	1.14:	+0.28	-1.5	48	-1.7:
7091	0.825	L	1.16	1.01	+0.13	-1.2	43	-1.4
5616	0.981	L**	1.08:	0.875:	+0.70:	-1.8:	33	-
		S**	0.96:	0.76:	+0.32:	-1.8:	28	-
5647	0.005	L**	1.11:	0.89:	+0.63:	-1.8:	37	-
7102	0.030	L**	1.13:	0.94:	+0.77:	-1.8:	16	-
		S	0.955	0.825	+0.02	-1.8	42	-0.9
6207	0.040	L**†	1.25:	0.965:	+0.62:	-1.8:	7	-
		S	1.095:	0.84:	-0.13:	-1.5:	33	-0.6:
5617	0.042	L	1.10:	0.88:	+0.12:	-1.8:	22	-1.2:
		S	0.945:	0.84:	-0.13:	-1.8:	31	-1.2:
6211	0.089	S	1.05	0.935	+0.34	-2.8	51	-1.3
5618	0.097	L**	1.36:	1.21:	+0.12:	-2.2:	26	-
		S	1.085:	0.95:	+0.13:	-1.8:	32	-1.2:
5651	0.123	-	1.235	1.00	+0.20	-2.8	65	-0.9
5556	0.196	-	1.21	1.07	+0.32	-2.8	52	-0.8
5058	0.358	-	1.215:	1.10:	+0.22:	-2.6:	38	+0.1:
7010	0.395	-	1.27	1.105	+0.37	-2.2	63	-1.0
7013	0.452	-	1.29	1.125	+0.22	-1.8	67	-0.8
7017	0.511	-	1.285	1.16	+0.24	-2.4	61	-0.7

Notes to Table 3

**Too few lines longward of λ4100 available for analysis. Results listed taken from Abt (1954); no attempt made to derive $[N_{Fe}]$.

†Numbers quoted based on Fe II.

make the analysis. Values of $[N_{Fe}]$ and other relevant curve-of-growth data are also listed in Table 3.

The Cepheid W Vir exhibits over the cycle a wide range of temperature and pressure; near light maximum, one finds $T_{ion} \sim 6300°$ K, $\log P_e \sim +1$; whereas near light minimum, $T_{ion} \sim 4000°$ K, $\log P_e \sim -2.5$. A test of the reliability of the abundance analysis is the requirement that $[N_{Fe}]$ be independent of changes in the atmospheric parameters around the cycle. In Figure 3 we exhibit $[N_{Fe}]$ as functions of θ_{exc} and phase ϕ. There is no systematic variation of $[N_{Fe}]$ with temperature (use of θ_{ion} instead of θ_{exc} would have introduced simply a zero-point shift in the figure), but a modest systematic effect appears as a function of phase in the sense that the Fe abundance is anomalously low on the rising branch of the light curve, especially in the spectra corresponding to the "longward-displaced" components. At these phases, the low regions of the atmosphere, where weak lines are formed, are disturbed by the passage of the pulsational wave (cf. Abt 1954), and it is the weak lines that play the greatest role in the abundance determination. We return to this point later (§§ III and IV). Omitting the one low-weight point with $[N_{Fe}] = +0.1$, we obtain $\langle [N_{Fe}] \rangle = -1.05 \pm 0.3$ (m.e.); omitting also the four points marked "L," we obtain $\langle [N_{Fe}] \rangle = -0.95 \pm 0.2$ (m.e.). From the coarse-analysis point of view, there is not much doubt that the Fe abundance per gram of stellar material is down by one order of magnitude from the solar value.

Abundances of spectroscopically conspicuous metals other than Fe were obtained from an analysis of three spectrograms well distributed in temperature, viz., Ce 6211, Ce 5651, and Ce 7010. Since Abt (1954) published only a few line strengths other than those for Fe I and Fe II, we reanalyzed the line intensities from microphotometer tracings. For each plate we adopted the simplified procedure of preparing a curve of line depth versus equivalent width based on Abt's measurements of Fe I and Fe II lines; the curve was entered with the depths of lines for other elements and the corresponding values of $\log W/\lambda$ read out. All line strengths are therefore essentially on the system of Abt; a catalog is given in Table 4.

The abundances derived from the three spectrograms are summarized in Table 5; for each element, we give also the number n of neutral and/or ionized lines measured, and a quality designation ("a" = good, "b" = fair, "c" = poor) based largely on n. The leading conclusion is that, while most of the iron-peak elements (except Sc) have abundances similar to Fe, elements such as Sc, Sr, Y, Zr, Ba, and Ce have abundances reduced below the solar value by yet another order of magnitude. In the context of nucleosynthesis theory (Burbidge *et al.* 1957), we can separate the elements formed by

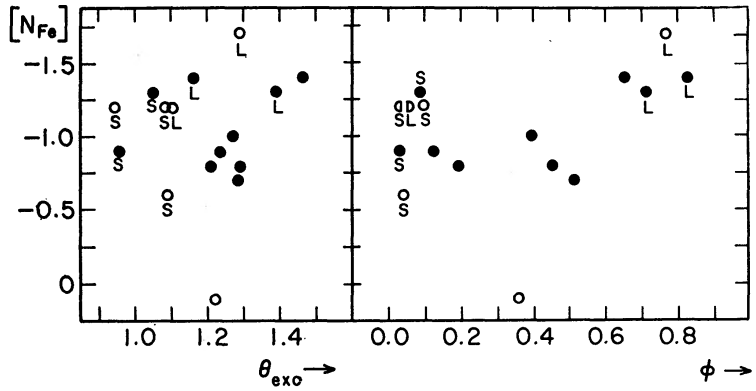

FIG. 3.—Values of $[N_{Fe}]$ as a function of θ_{exc} and ϕ in W Vir. Open circles are derived from Fe I curves of growth having fewer than forty lines and are assigned half-weight. For spectrograms obtained between $\phi = 0.70\ P$ and $0.10\ P$, "L" and "S" refer to material ahead of and behind the shock front, respectively (see § IV).

TABLE 4

EQUIVALENT WIDTHS OF LINES OTHER THAN Fe I and Fe II

Line (λ)	Ident.	log $\eta_\odot$	-log(W/λ) Ce 6211(S) φ=0.089 P	Ce 5651 φ=0.123 P	Ce 7010 φ=0.395 P	χ e.v.
4077.71*	Sr II	3.77	4.03	4.07	3.75	0.00
4215.52*	Sr II	3.30	4.31	4.22	3.84	0.00
4226.73*	Ca I	4.58	4.06	4.07	3.91	0.00
4246.83*	Sc II	2.93	4.54	4.63	4.26	0.31
4337.94	Ti II	2.75	-	-	4.10:	1.08
4341.40	Ti II	2.44:	-	-	4.26:	1.11
4349.80	Ce II	-0.30			5.62	0.70
4355.08	Ca I	1.82	5.82:	5.33:	5.40	2.70
4374.46	Sc II	1.90	4.72	-	-	0.62
4386.82	Ti II	0.70	4.71	4.52	4.52	2.59
4394.07	Ti II	1.38	4.43	4.41	4.38	1.22
4395.03	Ti II	2.37	3.94:	4.14:	3.98	1.08
4395.84	Ti II	1.17	4.09:	4.30:	4.40:	1.24
4398.30	Ti II	0.28	5.17	4.68	4.70	1.22
4403.28	Zr II	0.75	5.74:	5.75	5.58	1.18
4411.11	Ti II	0.80	4.79	4.69	4.72	3.08
4411.94	Ti II	0.80	5.17	4.67	4.72	1.22
4417.71	Ti II	1.70	4.20	4.43:	4.16	1.16
4421.95	Ti II	0.52:	4.83	4.67:	4.70	2.05
4425.45	Ca I	2.45	5.11	4.79	4.66	1.87
4435.66	Ca I	2.23	5.50:	4.42:	4.35	1.88
4436.29	Mn I	0.30	5.75	5.85	5.54	2.91
4441.72	V I	1.09	5.39::	4.65:	4.50	0.27
4443.81	Ti II	2.36	4.28:	4:32:	3.98	1.08
4468.49	Ti II	2.26	4.13	4.32	4.03	1.13
4477.07	Cr I	-0.30	-	6.40:	-	2.70
4485.39	Zr II	-	-	-	5.70:	1.23
4486.90	Ce II	0.10	5.50	6.04	5.60	0.29
4493.53	Ti II	0.28	5.36	4.73	4.67	1.08
4502.25	Mn I	0.92	>5.13:	5.31	5.60	2.91
4507.23	Cr II	0.05	5.41	6.26	5.58	3.09
4512.78	Ti I	0.90	5.79	5.83	5.21	0.83
4533.24	Ti I	1.50	5.46::	4.69:	4.77	0.84
4534.78	Ti I	1.35	-	4.72:	4.87:	0.83
4545.14	Ti II	0.84	4.97	5.06	4.63	1.13
4545.97	Cr I	1.31	-	5.61	5.38	0.94
4548.78	Ti I	1.09	-	5.51:	5.17::	0.82
4554.04	Ba II	2.80	4.34	4.30	4.06	0.00
4554.99	Cr II	0.48	5.27:	5.17:	4.83	4.05
4558.66	Cr II	1.18	4.69	4.60	4.46	4.06
4562.38	Ce II	0.18	5.65	5.40	5.23	0.00
4563.78	Ti II	2.15	4.21	4.29	4.09	1.22
4568.30	Ti II	0.28	5.83:	5.12	4.78	1.22
4571.09	Mg I	0.78	5.50	5.01:	4.43	0.00
4572.00	Ti II	2.27	4.20	4.28	4.07	1.56
4585.84	Ca I	1.77	5.57	4.94	4.98	2.57
4588.18	Cr II	1.12	4.62	4.85	4.57	4.05
4589.96	Ti II	0.48	4.51	4.55	4.31	1.23
4591.45	Cr I	1.01	5.63	5.97	5.28:	0.96
4605.03	Ni I	1.03	5.50:	5.30	5.35	3.47

TABLE 4 (continued)

Line (λ)	Ident.	log $\eta_\odot$	-log(W/λ) Ce 6211(S) φ=0.089 P	Ce 5651 φ=0.123 P	Ce 7010 φ=0.395 P	χ e.v.
4609.33	Ti II	0.03:	5.65:	5.67:	5.04	1.18
4613.92	Zr II	0.24	5.83	5.95	5.56	0.97
4617.27	Ti I	0.89	5.09:	5.73	5:41:	1.74
4618.80	Cr II	0.95	4.98	5.00	4.58	4.06
4623.10	Ti I	0.62	5.43	5.84	5.50	1.73
4626.07	Cr I	1.20	-	5.31	5.03	0.96
4628.18	Ce II	0.14	-	5.72	5.24	0.04
4634.08	Cr II	0.88	4.89	5.01	4.60	4.05
4636.32	Ti II	0.12	4.89	5.06	4.82	1.16
4639.39	Ti I	0.48	-	5.79	5.38:	1.73
4639.70	Ti I	0.48	-	6.22:	5.43:	1.74
4639.95	Ti I	0.38	-	6.30:	5.57:	1.73
4646.19	Cr I	1.38	-	-	4.71::	1.03
4647.96	Cr I	0.44	-	-	5.45:	2.53
4651.28	Cr I	1.08	5.54	5.49	5.11	0.98
4652.10	Cr I	1.26	-	5.21	5.11	1.00
4656.45	Ti I	1.00	5.95	5.65:	5.30:	0.00
4682.00	Ti I	1.28	5.47	5.12	5.22	0.05
4682.36	Y II	0.36	5.64	6.05	5.49	0.41
4702.97	Mg I	3.55	4.62	4.61	4.38	4.33
4707.99	Cr I	0.84	5.84	-	5.42:	3.15
4708.73	Ti II	0.64	5.17	-	4.58	1.23
4715.77	Ni I	1.12	-	5.46	-	3.53
4718.40	Cr I	0.98	5.56	5.78	5.60	3.18
4719.41	Ti II	0.00	5.63	5.71	5.04	1.24
4722.20	Zn I	1.00	4.96	5.13	4.94	4.01
4730.04	Mg I	-0.50	5.74	5.61:	5.50	4.33
4754.03	Mn I	1.85	5.17	4.79	4.76	2.27
4758.12	Ti I	0.41	5.77	5.79	5.48	2.24
4759.30	Ti I	0.57	-	5.58	5.45::	2.25
4763.89	Ti II	1.25	-	4.60	4.74	1.22
4764.56	Ti II	0.35	5.13	5.01	4.67	1.23
4777.68	Cr II	-0.75	-	5.58	5.41	3.81
4779.95	Ti II	1.14	5.13	4.74	4.49	2.04
4783.40	Mn I	2.42	-	4.98	4.60	2.29
4801.06	Cr I	1.51::	-	5.59	5.29	3.11
4805.18	Ti II	1.60:	-	-	4.48	2.05
4812.33	Cr II	0.70	-	-	5.02	3.85
4824.17	Cr II	1.40	-	4.88	4.60	3.85
4825.02	Cr II	-0.05	-	-	5.23	3.81
4836.19	Cr II	0.29	-	-	5.29	3.84
4840.97	Ti I	1.01	-	5.45	5.18	0.90
4848.27	Cr II	0.78	-	4.67	4.58	3.85
4849.10	Ti II	0.32	-	-	4.64	1.13
4874.12	Ti II	0.36:	-	-	4.97	3.08
4883.78	Y II	0.90	-	-	5.34	1.08
4884.62	Cr II	0.23	-	-	5.00	3.84
4900.11	Y II	1.01	-	4.80	5.10	1.03
4934.09	Ba II	2.80:	-	-	4.49	0.00
4942.50	Cr I	1.40	-	-	5.31	0.94
4964.93	Cr I	0.46	-	-	5.25:	0.94

*Notes: (-log W/λ) taken from Abt (1964).
Colons indicate low weight; double colons, very low weight.

TABLE 5

ABUNDANCES OF METALS IN W VIRGINIS

Element	B^2FH Process	Ce 6211		Ce 5651		Ce 7010		Mean
		$[N_{el}]$	$(N_{neut},N_{ion},qual.)$	$[N_{el}]$	$(N_{neut},N_{ion},qual.)$	$[N_{el}]$	$(N_{neut},N_{ion},qual.)$	$[N_{el}]$
Mg	He,α	-1.2	(2, 0, c)	-	-	-0.9	(2, 0, c)	-1.0
Ca	α	-1.9	(4, 0, b)	-1.0	(4, 0, b)	-1.5	(4, 0, b)	-1.5
Sc	s	-2.6	(0, 1, c)	-3.1	(0, 1, c)	-2.6	(0, 1, c)	-2.8
Ti	α,r	-1.3	(7, 24, a)	-1.1	(14, 24, a)	-1.1	(12, 28, a)	-1.2
Cr	e	-1.4	(4, 6, a)	-1.3	(8, 9, a)	-1.2	(10, 13, a)	-1.3
Mn	e	-0.8	(3, 0, c)	-0.6	(1, 0, c)	-1.5	(4, 0, b)	-1.0
Fe	e	-1.26	(51, 15, a)	-0.86	(65, 17, a)	-0.97	(63, 17, a)	-1.03
Ni	e	-	-	-0.8	(2, 0, c)	-	-	-0.8
Sr	s	-2.1	(0, 2, c)	-1.7	(0, 2, c)	-1.8	(0, 2, c)	-1.8
Y	s	-2.1	(0, 1, c)	-2.1	(0, 2, c)	-2.6	(0, 3, b)	-2.3
Zr	s	-2.2	(0, 2, c)	-2.3	(0, 2, c)	-2.5	(0, 2, c)	-2.3
Ba	s	-2.2	(0, 1, c)	-1.3	(0, 1, c)	-2.3	(0, 1, c)	-1.9
Ce	s	-1.7	(0, 2, c)	-2.0	(0, 3, c)	-2.0	(0, 4, b)	-1.9
"non-s"		-1.3		-1.0		-1.2		-1.1
"s"		-2.1		-2.1		-2.3		-2.2

the *s*-process from those formed by other processes. We obtain from the three plates the following mean results: $[N_{\text{non-}s}] = -1.1 \pm 0.1$ (p.e.) and $[N_s] = -2.2 \pm 0.2$ (p.e.). A similar excessive deficiency of *s*-process elements relative to Fe was found by Rodgers and Bell (1963) in κ Pav, and may be characteristic of numerous old stars of Population II (cf. Greenstein 1970). Segregation, for example, of Preston's (1961) abundances for RR Lyr, which has a metal deficiency similar to that of W Vir, yields $[N_{\text{non-}s}] = -1.3$ and $[N_s] = -1.7$; the latter quantity, however, is derived from only nine lines distributed over four elements, and the distinction may not be significant.

Any *s*-process elements that might have been produced in the central core of W Vir during evolution have apparently not been mixed into the atmosphere, despite the presumption that the star has undergone helium flashing. Evidently the present abundances reflect the mix in the primeval interstellar medium.

If the metal abundances are really as low as claimed here, then we should be able to detect the effect visually in weak lines by intercomparing spectrograms of W Vir with Type I supergiants of similar temperature. This is illustrated in Figure 4 (Plate 3); one can clearly see that, in passing from any of the Population I stars shown to W Vir, metallic lines of moderate intensity are little affected, but weak lines tend to disappear. The effect can be seen because even in the metal-rich stars, at the level where the weak metallic lines are formed, the continuous opacity has a 25 percent contribution from Rayleigh scattering on H, and of the H^- opacity about one-third of the free electrons are supplied by the ionization of H itself. A substantial part of the continuous opacity is due only to hydrogen, and therefore the change in the ratio of line to continuous opacity with decreasing metal abundance is readily discernible from simple visual inspection.

III. FINE ANALYSIS

As a check on the results of coarse analysis, and particularly the propriety of using Preston's "device" in stars of reduced metal abundance, we have calculated line intensities directly by means of an LTE fine analysis. Several LTE flux-constant, nonblanketed model atmospheres were kindly supplied by Drs. Duane Carbon and R. Hillendahl. All had $T_e = 5200°$ K; we selected two subcases: (1) $\log g = 1.0$, normal metals; and (2) $\log g = 0.0$, one-tenth normal metals. The former applies to the classical 45-day Cepheid SV Vul (see Fig. 4) near minimum light (Kraft *et al.* 1959; Parsons and Bouw 1970), the latter to W Vir at phase about $0.35P$ (see § IV for a discussion of $\log g$). The line intensities of W Vir change almost not at all between $\phi = 0.35P$ and $0.40P$; therefore, we can use the models to predict line strengths for Ce 7010.

Contribution functions, following Pecker (1950, 1951) as modified in practice by Aller, Elste, and Jugaku (1957), were computed for four lines of Fe I, one line of Fe II, and one line of Ti II. Two of the Fe I lines are "weak" or "moderately weak," two Fe I lines are on the flat portion of the curve of growth as are the Ti II and Fe II lines, and a range of lower excitation potentials is represented. The lines chosen are listed in Table 6. The contribution function C is defined by the following equations:

$$W\lambda/\lambda = \int_{-\infty}^{\infty} C(x)dx\,, \tag{2}$$

$$C(x) = MZ(x)\,\Psi G_{4550}(x)\,, \tag{3}$$

where $x = \log \tau_{4550}$, $MZ(x)$ is a state population factor determined locally in LTE by the assumed abundances, temperature, and pressure, $G_{4550}(x)$ is a weight factor describing the source function (taken here as Planckian), and Ψ is Pecker's saturation function (depending in turn on M and Z) which we assumed corresponded to the purely Doppler case (no pressure broadening). The reader is referred to the exhaustive paper by Aller *et al.* (1957) for details, and it is enough here to remark that a plot of C as a function of x displays the region of the atmosphere responsible for the line. Normally C peaks as x

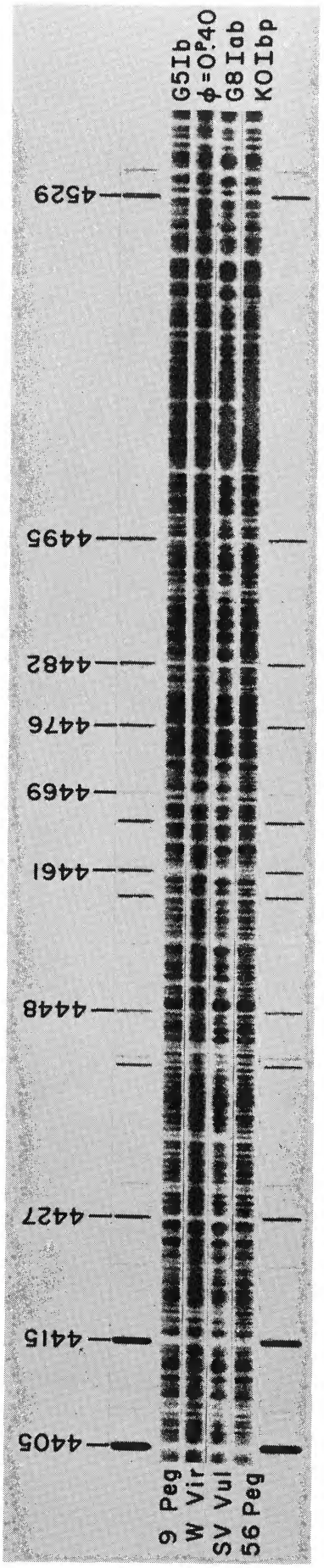

FIG. 4.—A portion of the spectrum of W Vir at $\phi = 0.40$ P compared with supergiants of similar T_e. SV Vul is a classical Cepheid of period 45 days. The values of T_e for 9 Peg, SV Vul, and 56 Peg are 5200°, 5040°, and 4900° K, respectively. Line weakening for fainter absorption lines in W Vir is especially noticeable between λλ4427 and 4448, and longward of λ4495.

BARKER *et al.* (*see* page 78)

TABLE 6

OBSERVED AND COMPUTED EQUIVALENT WIDTHS FOR SIX LINES OF Fe I, Fe II, AND Ti II

LINE (Å)	IDENTIFICATION	χ (eV)	$-\log W/\lambda$ (observed)	$-\log W/\lambda$ (computed)		$\log(W/\lambda)_{obs}-\log(W/\lambda)_{comp}$	
				Model 1	Model 2	Model 1	Model 2
4494.57.....	Fe I	2.19	4.33	4.35	4.44	+0.02	+0.11
4495.99.....	Fe I	3.64	5.47	4.53	5.14	−0.94	−0.33
4574.24.....	Fe I	3.20	>5.58	4.96	5.92	<−0.62	<+0.34
4489.74.....	Fe I	0.05	4.53	4.38	4.46	−0.15	−0.07
4582.83.....	Fe II	2.83	4.47	4.31	4.39	−0.16	−0.08
4545.14.....	Ti II	1.13	4.63	4.24	4.29	−0.39	−0.34

grows larger; for weak lines, $\Psi = 1$ and C declines eventually in response to the source function weight factor G. For saturated lines, in the present case, G plays a minor role because the rate of change of the source function with x is extremely small; rather, C declines because of the influence of Ψ. For these saturated lines, the computed equivalent width is quite insensitive to the assumed metal abundance, as would be expected.

We estimated the abundance of Fe by attempting to reproduce the observed equivalent widths of the two weak Fe I lines λλ4495.99 and 4574.24. These lines (see below) are formed so low in the atmosphere that departures from LTE are expected to be minimal. We adopted the solar Fe abundance favored by the Kiel group (Garz *et al.* 1969) and correspondingly reduced the values of gf given by Abt (1954) which were based on the earlier work by King and King (1938). Since only Nf enters, the line absorption coefficient is invariant to these changes. The recent adjustment in the Fe abundance affects the present work only through the model atmosphere, since Fe is a modest contributor to the free electron supply. However, adjustment of the Abt gf-values downward by a factor of 10 does permit a comparison with the most recent laboratory f-values for two of the lines, viz., λλ4494.57 (Bridges and Wiese 1970) and 4574.24 (Garz *et al.* 1969), and the agreement is found to be very good.

In the upper panels of Figure 5 we plot the leading parameters of the two models, viz., T, $\log P_e$, and $\log \kappa_{4550}$ as a function of x, and in the lower panels the corresponding contribution functions C for the six lines. Comparison of Figure 5 with Table 6 reveals that the computed equivalent widths of two weakest Fe I lines are about an order of magnitude greater than is observed in W Vir if the Fe abundance is taken as the solar value; if the Fe abundance is reduced by a factor of 10, quite reasonable agreement is obtained. Unfortunately, $\log W/\lambda$ for the weakest line λ4574.24 cannot be measured very accurately because of blending, but the ***upper bound*** to its equivalent width is 4 times smaller than the computed strength if normal Fe abundance is taken.

Inspection of Figure 5 gives one some insight into the meaning of the physical parameters used in curve-of-growth analyses. In practice, T_{exc} involves measurement of equivalent widths for moderate to moderately weak lines, i.e., those with $\log W/\lambda > -5.10$. (The weakest lines usually do not include a sufficiently large sample of lines of low excitation.) This favors the low temperature plateau above $\log \tau_{4550} = -1$ as a region representative of T_{exc}, and it matters little where the line is formed; the temperature and continuous opacity are essentially constant. For the phase of SV Vul illustrated in Figure 5, for example, one has $T_e = 5040°$ K corresponding to G8 Ib (Kraft 1961), and $T_{exc} = 4000° \text{ K} \pm 300°$ K (Kraft *et al.* 1959); the latter agrees well with the mean plateau temperature of 4240° K in Model 1.

For the same star, Kraft *et al.* derived $T_{ion} = 4630°$ K, a temperature reached in

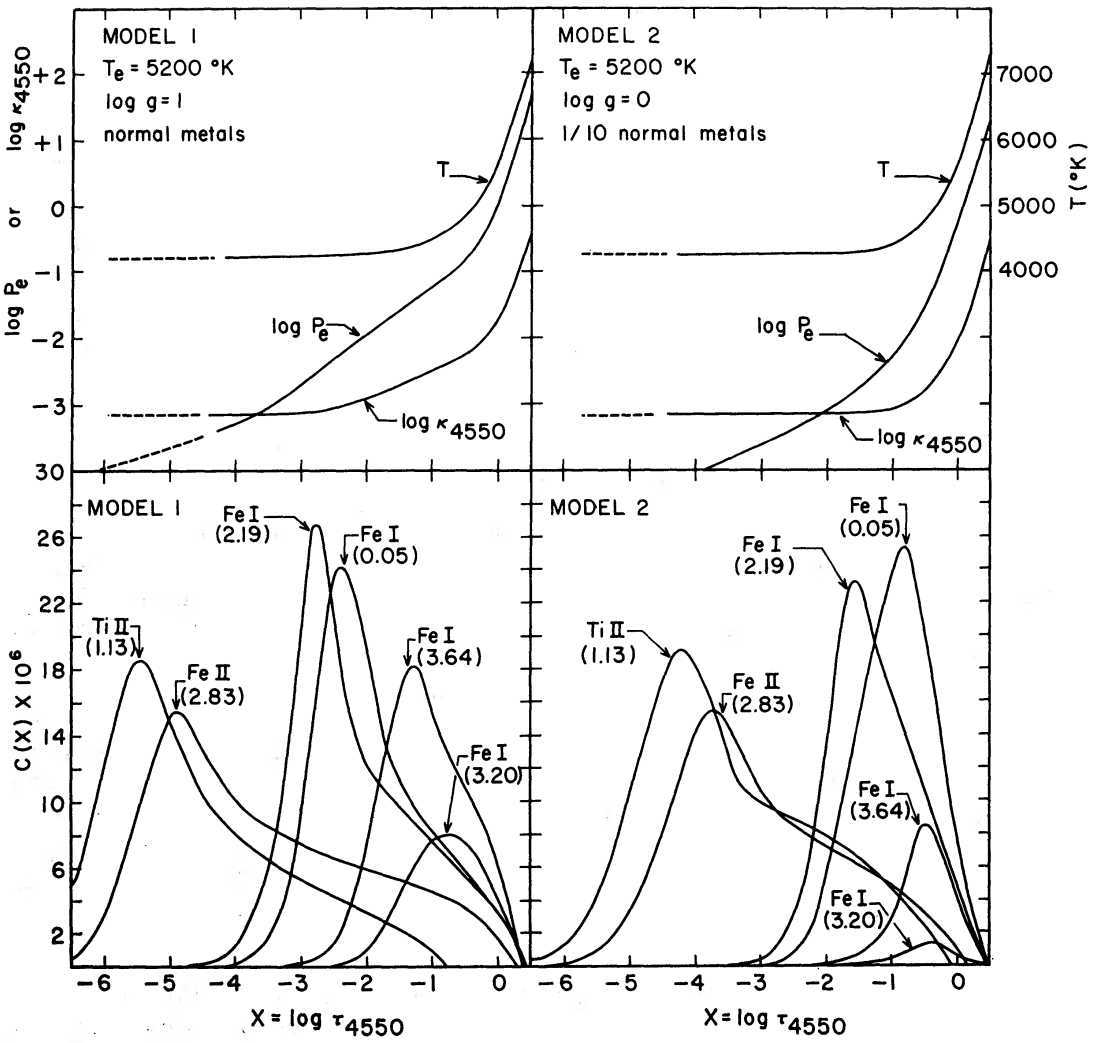

FIG. 5.—Model-atmosphere parameters and contribution functions for lines of Fe I, Fe II, and Ti II. LTE model atmospheres are those computed by Carbon. *Dashed lines*, extrapolations based on calculations by Hillendahl. A number in parentheses is the lower excitation potential of the transition (in volts).

Model 1 at log τ_{4550} near -0.75. Now we may rewrite equation (1) as follows, as long as the degree of ionization of Fe is high:

$$Q(T_{\rm ion}) \equiv [\kappa_\lambda] + \log S \equiv [N_{\rm Fe}] - \left[\frac{N_{\rm Fe\ I}}{\kappa_\lambda V}\right] - [V], \qquad (4)$$

where log S is the shift of the Fe II curve of growth onto the Fe I curve of growth. The left-hand side of equation (4) depends only on $T_{\rm ion}$, as long as the major source of opacity remains H^-. This is because κ_λ goes directly as P_e, and S goes inversely. Thus for a fixed value of $[N_{\rm Fe}]$, $Q(T_{\rm ion})$ depends principally on the value of $[N_{\rm Fe\ I}/\kappa_\lambda]$ at the level in the atmosphere where the weak and moderately weak Fe I lines (i.e., those with log $W/\lambda < -5.00$) are formed, since these lines carry the greatest weight in shifting the stellar onto the solar curve of growth. For Model 1, such lines are formed between log $\tau_{4550} = -0.75$ and -0.50 where the mean temperature is 4750° K. This is quite close to the value of $T_{\rm ion}$ derived from the spectroscopic analysis cited above for SV Vul. On the other hand,

in Model 2 with reduced metal abundances, Fe I lines of this strength are formed at essentially the same optical depth as in Model 1. This is because the weight factor $G(x)$ is nearly the same in the two models as a consequence of the near equality in temperature distribution. Thus the temperature at which the weak Fe I lines are formed in Model 2 is not more than 100° K different from the temperature in Model 1. The plateau temperatures in the two models are the same, but in Model 2, the moderately weak to moderate Fe I lines are formed somewhat lower than they are in Model 1; thus $T_{\rm exc}$ (Model 3) $-$ $T_{\rm exc}$ (Model 1) = 150° K, a small deviation. Thus if our interpretation of $T_{\rm ion}$ is correct and is about the same for the two models, then our application of the Preston "device" to the case of W Vir, to the extent its atmosphere can be represented by Model 2, seems justified.

It is not known in principle if the preceding analysis would be seriously upset by departures from LTE, but it is not likely to be disturbed by stratification effects such as increase in turbulence with height. The Fe abundance derived from curves of growth depends on rather weak lines of Fe I; and because $[N_{\rm Fe\ I}/\kappa V]$ is not a function of P_e in the first order, it is independent of the degree of ionization (as long as it is high). Whatever the region of formation of the Fe II lines, departures there from LTE or from other assumptions inherent in the fine analysis are not likely to affect the Fe abundance significantly. In the case of W Vir, the issue may not arise in any case. The narrowness of the core of Hα suggests either that, high in the atmosphere, the microturbulent velocity does not exceed the photospheric value, or that LTE is a good approximation at all heights, or both. The first possibility at least is supported by the fact that the Ti II lines, weak and strong, can be fitted with the same curve of growth as the Fe I lines at $\phi = 0.40P$ (Ce 7010).

IV. RADIUS VARIATIONS; TEST OF THE SHOCK-WAVE MODEL

Kwee (1967*c*, 1968) derived the mean absolute magnitude of W Vir by comparing it with Cepheids in globular clusters. His photometry (1967*a*, *b*) and analysis, based in part on work by Arp (1955), yield $\langle V \rangle = 9.93$ and $\langle M_V \rangle = 2.40$. In Table 7 we list effective temperatures, colors, magnitudes, bolometric corrections, and radii as a function of phase. We derived the values of T_e from $T_{\rm ion}$, using the Kraft-Parsons-Bouw transformation, as explained in § II*a*. Between $\phi = 0.10P$ and $0.65P$, however, $T_{\rm ion}$ was not derived directly from $T_{\rm exc}$. Rather, we assigned the mean Fe abundance, $[N_{\rm Fe}] = -1.0$, to each Mount Wilson spectrogram analyzed, made use of equation (4), and from a plot of $T_{\rm ion}$ as a function of phase derived the smoothed values given in the table. In the phase interval 0.65–$0.10P$, the atmosphere is composite, with the "longward-displaced" (L) components of the absorption lines arising in a region higher in the atmosphere than the region responsible for the "shortward displaced" (S) components (Abt 1954). As discussed below, the velocity discontinuity responsible for the line splitting is above the level of the photosphere from phase $0.65P$, at least until evidence for its existence disappears at phase $0.10P$. Since the region ahead of the discontinuity is transparent in the continuum (Abt 1954), we need to make estimates of $T_{\rm ion}$ for the region behind the discontinuity if we are to obtain T_e. However, physical conditions there are not known because of the small number of lines that can be measured for coarse analysis. At maximum light and continuing to phase $0.10P$, the S components dominate the spectrum, and T_e has been estimated from $T_{\rm ion}$ as before.

We resorted to the colors to obtain an estimate of T_e at one phase between 0.65 and $0.00P$. At phase $0.85P$, $(B - V) = +0.65$. This color is affected by absorption-line blanketing in the overlying region. From the blanketing theory for main sequence F- and G-type stars (Wildey *et al.* 1962), we estimate that a star with $[N_{\rm Fe}] = -1.0$ will have $(B - V)$ reddened by 0.12 mag in comparison with a line-free star. Ignoring interstellar reddening, we find a true $(B - V) = +0.53$, which by comparison with the descending branch of the color curve gives the same T_e as at phase 0.08 P, viz., 5600° K (the L com-

TABLE 7

EFFECTIVE TEMPERATURE, LUMINOSITY, COLOR, AND RADIUS

OF W VIR AS A FUNCTION OF PHASE

Phase(P)*	$(B-V)_{obs}$ (Kwee)	T_{ion} (°K)	T_e (°K)	B.C. (Johnson)	M_v	M_{bol}	R x 10^{-6}km
0.00	0.45	6270(S)	6470	+0.10	-2.80	-2.70	16.7
0.05	0.52	5770(S)	6000	+0.07	-2.78	-2.71	19.2
0.10	0.57	5150(S)	5310	-0.08	-2.77	-2.85	26.5
0.15	0.61	4760	5040	-0.15	-2.78	-2.93	30.0
0.20	0.65	4550	4830	-0.24	-2.75	-2.99	34.0
0.25	0.68	4520	4800	-0.25	-2.74	-2.99	34.1
0.30	0.71	4470	4760	-0.26	-2.71	-2.97	34.5
0.35	0.73	4450	4740	-0.27	-2.66	-2.93	34.5
0.40	0.78	4380	4660	-0.30	-2.52	-2.82	33.7
0.45	0.83	4180	4420	-0.42	-2.29	-2.71	35.8
0.50	0.90	4030	4280	-0.52	-2.05	-2.57	35.9
0.55	0.96	4060	4320	-0.48	-1.81	-2.29	31.0
0.60	0.99	4180	4420	-0.42	-1.64	-2.06	26.5
0.65	0.94	4380	4660	-0.30	-1.64	-1.94	22.5
0.70	0.87	-	4880:	-0.22	-1.78	-2.00	21.0:
0.75	0.80	-	5110:	-0.13	-1.91	-2.04	19.6:
0.80	0.72	-	5380:	-0.07	-2.08	-2.15	18.7:
0.85	0.65	-	5620:	-0.01	-2.24	-2.25	17.7:
0.90	0.54	-	5940:	+0.05	-2.44	-2.39	17.1:
0.95	0.46	-	6310:	+0.09	-2.63	-2.54	16.3:
0.98	0.43	-	6550:	+0.11	-2.74	-2.63	15.4:

*Counted from maximum light in B

ponents at phase $0.08P$ are feeble and produce negligible blanketing). We interpolated the values of T_e listed in Table 7 from the estimates at phases 0.65, 0.85, and $0.00P$.

Bolometric corrections were taken from the list by Johnson (1966), with T_e rather than $(B - V)$ as argument, since line blanketing is known to have only a small effect on the V-magnitude of a star with given T_e and M_{bol} (Wildey *et al.* 1962). The derived radii, listed in Table 7, are illustrated (after smoothing) as a function of phase in Figure 6. Between $\phi = 0.70P$ and $0.00P$, the curve is uncertain, and minimum radius is unknown in magnitude by $\sim\pm 10$ percent and in phase by $\pm 0.05P$. There is little doubt that maximum radius occurs near $\phi = 0.40P$, and that the radius variation is $\sim\pm 40$ percent of a mean value near 26×10^6 km. Maximum bolometric luminosity is at phase $0.25P$. We assume that the radius changes shown in Figure 6 describe the motion of the stellar photosphere.

At phase $0.40P$, when the fundamental plate Ce 7010 was obtained, the photospheric radius is about 35×10^6 km, and for a mass of $0.65\,\mathfrak{M}_\odot$ (the evolutionary value suggested by Schwarzschild and Härm 1970) the surface gravity is 7.1 cm sec^{-2}. In the regions where the spectral lines are formed, the change in radial velocity (Abt 1954) indicates that the gravity should be reduced by an $\ddot{r}$ term of 5.5 cm sec^{-2}, so that the effective $\log g = +0.2$. A similar value $\ddot{r}$ would be obtained from the change in photospheric radius. The selection of $\log g = 0$ from among the model atmospheres discussed in § III therefore appears justified.

From these static model atmospheres, the abundances of §§ II and III, and the photospheric radii we can make a test for plausibility of the shock-wave model. In this picture, a shock front is to be associated with the hydrogen emission lines that first make an appearance in the spectrum at phase $0.65P$. At this moment, the shock lies at a level corresponding to the photosphere. The front rises and the preshocked material becomes optically thin in the continuum; at phase $0.825P$, double absorption lines appear. The shortward (S) and longward (L) components arise in material behind and ahead of the

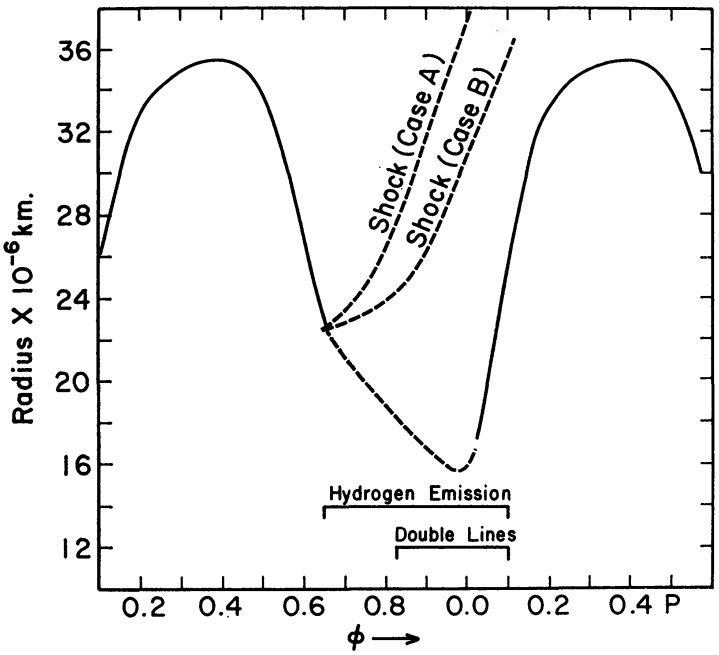

FIG. 6.—Radius variations of W Vir. R is derived from $L = 4\pi R^2 \sigma T_e^4$, and is assumed to represent the motion of the stellar photosphere. Phases are counted from blue (B) light maximum. Dashed section is uncertain because of uncertainties in T_e, as explained in the text. The motion of the strong shock front is shown for two choices of the center-of-mass velocity of the star.

shock, respectively. The shock front rises above the photosphere, consuming the preshocked material before it, and the longward absorption components gradually disappear. By phase $0.10P$, all traces of the preshocked material have disappeared and the emission lines are gone.

We can test this model by the requirement that the height H of the atmosphere above the shock be the same as the distance D traveled by the shock from phase $0.65P$ to phase $0.10P$. H can be estimated from Model 2 of § III, since at phase $0.65P$, T_e is only 150° cooler than it is at phase $0.40P$. The contribution functions (Fig. 5) show that significant line opacity can be expected as high as $\log \tau \sim -4$ to -5, and the model gives a height for this material above the photosphere of about 20×10^6 km, a number roughly equal to the radius of the photosphere itself. Since the layers overlying the shock front at phase $0.65P$ have a mean continuous opacity of order unity, we can also write $H \sim 1/\rho\langle\kappa\rangle$, where ρ is the density and $\langle\kappa\rangle$ the mean mass absorption coefficient determined from the analysis of plate Ce 5110. We obtain $\rho = 7.0 \times 10^{-10}$ gm cm^{-3}, $\langle\kappa\rangle = 1.6 \times 10^{-3}$ cm^2 g^{-1}, and $H = 10 \times 10^6$ km, in good agreement with the first estimate. These two estimates are rather independent since the former goes inversely as g and is independent of $[N_{\rm Fe}]$, whereas the latter depends directly on the metal abundances derived in this paper. Using the same procedure, Abt (1954) obtained $H = 0.3 \times 10^6$ km, about 30 times smaller than our value. His values of ρ and $\langle\kappa\rangle$ were both larger than ours, directly reflecting his assumption of a normal metal abundance.

The distance D traveled by the shock front can be obtained by integrating the radial velocities. We assume first that the center-of-mass velocity is given by the mean of the maximum and minimum velocities (Case A), in accordance with Wallerstein's (1959*a*) study of M5, Nos. 42 and 84. Between $\phi = 0.65P$ and $0.825P$, Abt was able to measure the emission velocity directly: when the absorption lines arising behind the front are first seen at phase $0.825P$, they have the same velocity as the emission lines; the shock therefore is "strong" and is characterized by a large pressure and density discontinuity (Courant and Friedrichs 1948). At this phase, however, the intensities of too few spectral lines arising in the wake can be measured to test this surmise. Later, the emission lines of hydrogen become too badly mutilated by overlying self-absorption to be measured reliably for radial velocity. Between phases $0.00P$ and $0.10P$, however, we can analyze the pressures and densities in material on both sides of the front. For the preshocked material (corresponding to the L components), the strengths of weak and moderately weak lines of Fe I, and therefore $[N/\kappa V]$, are poorly determined, both because they are mutilated by the underlying S components and because they tend to be formed mostly *behind* the front, as may be seen by inspection of the contribution functions (cf. Fig. 5). We therefore resorted to the Schuster-Schwarzschild approximation for the curve of growth of the L components, and derived the degree of ionization without reference to the Fe abundance. We estimated $T_{\rm ion}$ from $T_{\rm exc}$ using Preston's "device," and obtained $\log P_e$ from the shift of the Fe II onto the Fe I curve of growth, a procedure based essentially on moderately strong lines. Gas pressures P_g and densities ρ were estimated at all phases from $T_{\rm ion}$, P_e, and the hydrogen/metal ratio. In the present case, P_g and ρ are not easily determined, since the reduced metal abundance makes the relationship between P_e and P_g rather dependent on the degree of hydrogen ionization, a quantity in turn highly sensitive to small errors in $T_{\rm ion}$.

The variations in ρ and P_e around the cycle are shown in Figure 7. Although the errors are large, it seems rather certain that the density has an average value around 10^{-9} g cm^{-3}, reaches a minimum near maximum stellar radius, and exhibits a sharp discontinuity by a factor of 10 to 100 at the double-line phase. The shock is therefore "strong," and the velocity of the front is presumably the same as that of the material behind it. The velocity curve of the L components can therefore be integrated directly to obtain the distance D traveled by the front. We find from Abt's (1954) paper, $D = 19 \times 10^6$ km. If we had taken the systemic velocity so as to correspond to a general infall of material of (say) 9 km sec^{-1} (Case B), we would have had (Abt 1954) $D = 13 \times 10^6$

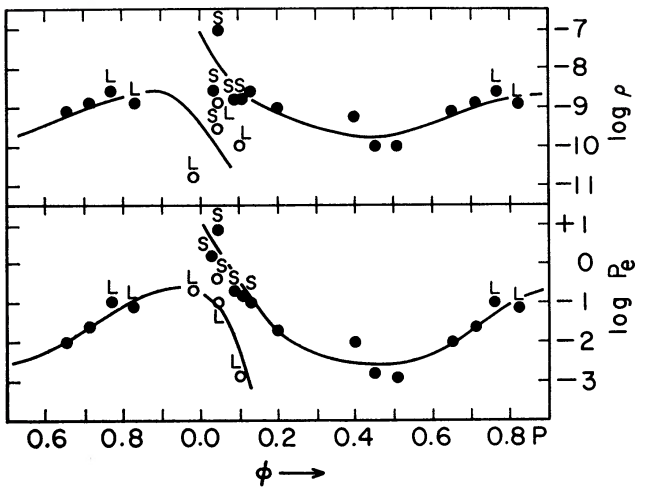

FIG. 7.—Variation of density (ρ) and electron pressure (P_e) around the cycle. Open circles have low weight. "S" and "L" refer to material behind and ahead of the shock front, respectively.

km. In any case, D agrees well with our two estimates of H, as is required of the shock-wave model. Wallerstein (1959*b*) suggested earlier that a reduction in metal abundance would support the shock-wave model by yielding $D \sim H$, a conclusion demonstrated here.

The location of the shock front in Cases A and B is shown in Figure 6. It is somewhat surprising (Castor 1970) that the photospheric advance lags so far behind the advance of the shock. The former might actually come much earlier than is indicated in Figure 6 if our values of T_e are too high between $\phi = 0.60\ P$ and maximum light. The photosphere would also follow the shock more closely if the systemic velocity were taken 10–20 km sec^{-1} more negative; this would, however, violate the rather limited results on radial velocities of Cepheids in globular clusters (Wallerstein 1959*a*).

Note added in proof, 1971 January 6.—Dr. George Wallerstein has kindly called our attention to two points, the second of which could somewhat affect the conclusions of this paper. (1) Scandium is no longer included among the *s*-process elements (cf. Arnett and Clayton, *Nature*, **227**, 780, 1970) by most workers in the field of nucleogenesis. However, since the weight of our Sc-abundance determination is quite low, its inclusion in $[N_{\text{non-}s}]$ in no way affects the conclusions of this paper. (2) Our metal abundances (with one exception) are fairly well correlated with the second ionization potentials in the sense that those metals with second ionization potentials above 13.54 eV have anomalously low abundances. The one exception is Ca [I.P. (Ca II) = 11.82 eV] for which the abundance, while a little low compared with Fe, Ti, and Cr, is considerably higher than that of the *s*-process group. The possibility that Sr, Y, Zr, Ba, Ce, and Sc are mostly doubly ionized as a result of emission in the Lyman continuum, while unlikely (owing to the result for Ca), cannot definitely be ruled out.

We are greatly indebted to Dr. R. Hillendahl of Ames Research Center and Dr. Duane Carbon of Harvard College Observatory for the use of model atmospheres computed by them, and to the Director of the Mount Wilson Observatory for the loan of plates of W Vir. We thank Mr. Remington Stone of Lick Observatory for obtaining photoelectric observations of W Vir from which Kwee's ephemeris was checked. One of us (R. P. K.) is grateful to the Joint Institute for Laboratory Astrophysics for the award of a Visiting Fellowship and wishes to record his special thanks to Dr. John Castor of JILA for valuable and illuminating discussions on shock-wave phenomena. Helpful talks on the evaluation of contribution functions were had also with Dr. F. Praderie.

REFERENCES

Abt, H. A. 1954, *Ap. J. Suppl.*, **1**, 63.
Aller, L. H. 1953, *Astrophysics* (New York: Ronald Press), p. 291.
Aller, L. H., Elste, G., and Jugaku, J. 1957, *Ap. J. Suppl.*, **3**, 1.
Aller, L. H., and Pierce, A. 1952, *Ap. J.*, **116**, 176.
Arp, H. C. 1955, *A.J.*, **60**, 1.
Bridges, J., and Wiese, W. 1970, *Ap. J.* (*Letters*), **161**, L71.
Burbidge, E., Burbidge, G., Fowler, W., and Hoyle, F. 1957, *Rev. Mod. Phys.*, **29**, 548.
Castor, J. 1970 (private communication).
Christy, R. F. 1966, *Ap. J.*, **145**, 337.
Courant, R. and Friedrichs, K. 1948, *Supersonic Flow and Shock Waves* (New York: Interscience Publishers), p. 154.
Edmonds, F., Schlüter, H., and Wells, D. 1967, *Mem. R.A.S.*, **71**, 271.
Garz, T., Holweger, H., Kock, M., and Richter, J. 1969, *Astr. and Ap.*, **2**, 446.
Greenstein, J. L. 1970, *Comments Ap. and Space Sci.*, **2**, 85.
Griem, H. R. 1964, *Plasma Spectroscopy* (New York: McGraw-Hill Book Co.), p. 92.
Gunn, J., and Kraft, R. 1963, *Ap. J.*, **137**, 301.
Johnson, H. L. 1966, in *Ann. Rev. Astr. and Ap.*, **4**, 193.
King, R., and King A. 1938, *Ap. J.*, **87**, 24.
Kraft, R. 1961, *Ap. J.*, **134**, 616.
Kraft, R., Camp, D., Fernie, J., Fujita, C., and Hughes, W. 1959, *Ap. J.*, **129**, 50.
Kraft, R., Preston, G., and Wolff, S. 1964, *Ap. J.*, **140**, 235.
Kwee, K. 1967*a*, *B.A.N. Suppl.*, **2**, 77.
———. 1967*b*, *ibid.*, p. 97.
———. 1967*c*, *B.A.N.*, **19**, 260.
———. 1968, *ibid.*, p. 374.
Oke, J. B. 1966, *Ap. J.*, **145**, 468.
Oke, J. B., and Searle, L. 1962, *Ap. J.*, **135**, 790.
Parsons, S., and Bouw, G. 1970, *M N.R A.S.* (in press).
Pecker, J. C. 1950, *Ann. d'ap.*, **13**, 319 and 433.
———. 1951, *ibid.*, **14**, 383.
Preston, G. 1961, *Ap. J.*, **134**, 507.
Rodgers, A., and Bell, R. 1963, *M.N.R.A.S.*, **125**, 487.
———. 1967, *ibid.*, **136**, 91.
Schmidt, E. 1970, *Ap. J.*, **162**, 871.
Schwarzschild, M., and Härm, R. 1970, *Ap. J.*, **160**, 341.
Searle, L., Oke, J. B., and Giver, L. P. 1962, *Ap. J.*, **136**, 393.
Searle, L., and Rodgers, A. 1966, *Ap. J.*, **143**, 809.
Wallerstein, G. 1959*a*, *Ap. J.*, **129**, 356.
———. 1959*b*, *ibid.*, **130**, 560.
———. 1970, *ibid.*, **160**, 345.
Wildey, R., Burbidge, E., Sandage, A., and Burbidge, G. 1962, *Ap. J.*, **135**, 94.
Wilson, O., and Bappu, M. K. V. 1957, *Ap. J.*, **125**, 661.